

Article

Ultra-Scratch-Resistant, Hydrophobic and Transparent Organosilicon-Epoxy-Resin Coating with a Double Cross-Link Structure

Zeyu Qiu ¹, Haofeng Lin ¹, Longlong Zeng ¹, Yunfeng Liang ¹, Chunhong Zeng ² and Ruijiang Hong ^{1,*} 

¹ Guangdong Provincial Key Laboratory of Photovoltaic Technology, Institute for Solar Energy Systems, School of Physics, Sun Yat-sen University, Guangzhou 510006, China; chouzy@mail2.sysu.edu.cn (Z.Q.); linhf27@mail2.sysu.edu.cn (H.L.); zengllong@mail2.sysu.edu.cn (L.Z.); liangyf36@mail2.sysu.edu.cn (Y.L.)

² School of Materials, Sun Yat-sen University, Guangzhou 510275, China; zengchh7@mail.sysu.edu.cn

* Correspondence: hongruij@mail.sysu.edu.cn

Abstract: In this paper, an ultra-scratch-resistant, hydrophobic and transparent coating was fabricated by the sol-gel method using (3-Glycidyoxypropyl) triethoxysilane (GPTES) and curing agents. When the silanol was condensed, the ring-opening reaction of the epoxy groups also took place, which formed a double-cross-linked network (Si-O-Si and R₃N). This network structure restricted the molecule chains from being twisted or dislocated, resulting in a great improvement of the abrasion resistance of the coating. A pencil hardness grade up to 8H was obtained. The coating also showed excellent stability after being soaked in pH = 2 and pH = 12 solutions, seawater and acetone, respectively. In addition, a water contact angle of 121° was obtained by post-treatment with hexamethyldisilazane (HMDS). The average transmittance of the coating reached to 90% in the wavelength range of 400–800 nm, nearly identical to the glass substrate. With multiple desirable properties and a simple fabrication process, this low-cost coating shows great potential in many practical applications.

Keywords: scratch-resistant; hydrophobic; GPTES; transparent; sol-gel



Citation: Qiu, Z.; Lin, H.; Zeng, L.; Liang, Y.; Zeng, C.; Hong, R. Ultra-Scratch-Resistant, Hydrophobic and Transparent Organosilicon-Epoxy-Resin Coating with a Double Cross-Link Structure. *Appl. Sci.* **2022**, *12*, 4854. <https://doi.org/10.3390/app12104854>

Academic Editors: Pijush Samui, Aydin Azizi, Ahmed Hussein Kamel Ahmed Elshafie, Yixia Zhang and Danial Jahed Armaghani

Received: 21 April 2022

Accepted: 10 May 2022

Published: 11 May 2022

Publisher's Note: MDPI stays neutral with regard to jurisdictional claims in published maps and institutional affiliations.



Copyright: © 2022 by the authors. Licensee MDPI, Basel, Switzerland. This article is an open access article distributed under the terms and conditions of the Creative Commons Attribution (CC BY) license (<https://creativecommons.org/licenses/by/4.0/>).

1. Introduction

Multifunctional transparent coatings are closely related to our lives and are categorized as one of the hot topics of many researchers [1,2]. While maintaining transparency, the coating is also endowed with multiple properties, such as self-cleaning [3,4], anti-fogging [5,6], oil-water separation [7], anti-corrosion [8–10], anti-reflection [11,12] and self-healing [13–15]. There are usually two ways to achieve self-cleaning, the super-hydrophilic surface and the super-hydrophobic surface. When water droplets come into contact with the coating, they will immediately be spread over the entire surface to form a continuous water film, thereby taking away the dirt on the surface [16]. The smooth surface that reduces the scattering of light makes the coating transparent and anti-fogging [5]. On the other hand, when the water droplets come into contact with the coating with low surface tension, the water droplets will keep their spherical shape and roll off quickly from the surface [17]. The preparation of superhydrophobic surfaces often relies on two factors, micro or nano-scaled hierarchical structures [18] and low surface energy materials [19]. In addition, a transparent coating is often used as a protective coating to protect metallic substrates from corrosion, because the dense and inert coating separates the metal from the environment [20]. Furthermore, anti-reflective coatings are often used in solar cells [12]. The refractive index of the antireflective coatings is lower than that of the substrate. Through the interference of light, it effectively reduces the reflection loss of incident light and improves the efficiency of solar cells [21]. What is more, the damaged structure can be recovered spontaneously by self-healing materials with external stimuli [15]. Self-healing coatings repair damage in two ways, inherent reversible noncovalent interactions [22–27] and dynamic covalent bonds [28–32].

However, these coatings are often soft and susceptible to scratches and abrasion. Scratches may make the surface rough, which will greatly cause the scattering of light, thereby reducing the transparency of the coating [33]. In addition, self-cleaning, anti-corrosion and other functions may also be affected, which severely restricts its application in daily life. Although the self-healing coating can relieve the effects of scratches to a certain extent, it cannot totally eliminate the damage of scratches [15]. Therefore, scratch resistance is also an important point for transparent coatings. Zhang et al. prepared a bilayer antireflective coating with the top layer of ultra-low refractive index from fully dispersing nano-silica particles by mixing HMDS and achieved an average transmittance of 99.90% in the visible region [34]. However, the coating with an ultra-low refractive index was usually rather soft, easily scratched. Mousavi et al. fabricated a transparent scratch-resistant coating through the direct oxidation of Al-coated glass [35]. After annealing at 600 °C, the pencil hardness of the coating increased to 9H due to the hard Al₂O₃ particles. However, the transmittance of the coating declined from 90% to 75%. Hua Zhou et al. prepared durable and superhydrophobic fabric coatings through simple mixtures of fluorinated silica nanoparticles and polydimethylsiloxane (PDMS) and showed that the water contact angle only decreased from 170° to 150° after 28,000 cycles of abrasion under 12 kPa [36]. However, the transparency of the coating was not mentioned.

In general, the epoxy resin needs to be solidified to increase its hardness [37–39] through a ring-opening reaction to form an organic network. (3-Glycidyloxypropyl) Trimethoxysilane (GLYMO) and (3-Glycidyloxypropyl) Triethoxysilane (GPTES) contain epoxy groups, as silane coupling agents, often used as surface hardening agents [37]. Zhi et al. provided a method to fabricate a durable superhydrophobic antireflection coating via introducing an organic network from KH560 and octadecylamine (ODA) [40]. In detail, the coating resisted scratches of a 4H pencil and the transmittance was 93%, which represented a 3% improvement of the uncoated substrate. Omer Kesmez et al. reported a hybrid organic–inorganic photocatalytic nanocomposite film, composed of Ce-doped TiO₂ nanoparticles and TEOS, GPTES, 1H, 1H, 2H, 2H-perfluorooctyl triethoxysilane [41]. This coating exhibited good transparency and the pencil hardness was >9H. Therefore, silane coupling agents containing epoxy groups can enhance mechanical damage resistance.

In this work, we prepare an ultra-scratch-resistant and hydrophobic polymer coating, based on a double-cross-link structure from GPTES and a curing agent, diethylenetriamine (DETA) or m-Xylylenediamine (MXDA). It protected the substrate from the scratches of an 8H pencil without deteriorating its transparency. The fabrication process of the coating, sol–gel method, is a simple and cost-effective thin film preparation method. It can be found that the coating was relatively durable after being soaked in different corrosive liquids. From the results of thermogravimetric analysis, it is also demonstrated that this polymer coating with a wide working temperature and hydrophobicity provided the possibility for practical applications on metal and/or wood surface.

2. Experimental Procedure

2.1. Materials

(3-Glycidyloxypropyl) Triethoxysilane (GPTES), hexamethyldisilazane (HMDS), tetraethyl orthosilicate (TEOS), methyltriethoxysilane (MTES), diethylenetriamine (DETA), m-xylylenediamine (MXDA) and ammonia (25~28%) were purchased from Shanghai Aladdin Biochemical Technology Co., Ltd., Shanghai, China. Anhydrous ethanol (EtOH), acetone, sodium hydroxide (NaOH) and sodium chloride (NaCl) were purchased from Tianjin Zhiyuan Chemical Reagent Co., Ltd., Tianjin, China. All the reagents used in this work were not purified further. High purity water was prepared by a Purescience water purification system.

2.2. Preparation of Coatings

2.2.1. Preparation of the DETA-Organosilicon-Epoxy-Resin (DETA-OSER) Coating and MXDA-Organosilicon-Epoxy-Resin (MXDA-OSER) Coating

GPTES (5.5 mL) was mixed with the EtOH (43.0 mL) with stirring for 30 min. Then, high purity water (1.0 mL) and DETA (0.8 mL) or MXDA (1.3 mL) were added to the solution and the mixture was stirred for 4 h. After stirring, the solution was transferred to a cool place to age for 7 days. After 7 days, the solution formed a sol. Then, EtOH (50 mL) was added to dilute the sol for later dip-coating.

Glass and silicon wafer were used as substrates to prepared samples for transmittance and refractive index measurement directly. The glass substrates were cleaned in an ultrasonic bath with high purity water, ethanol and acetone, respectively. After that, they were dried in the baker at 60 °C prior to dip-coating. The DETA-OSER coatings were dip-coated on glass substrates with a withdrawal rate of 1.5 mm/s. Then, the samples were immersed in HMDS for 3 days to obtain hydrophobic surface. Finally, the DETA-OSER-coated glasses were annealed in a muffle furnace at 160 °C for 1.5 h, and the MXDA-OSER-coated glasses were annealed in a muffle furnace at 155 °C for 1.5 h.

2.2.2. Preparation of the NH₃-Organosilicon-Epoxy-Resin (NH₃-OSER) Coating

GPTES (5.5 mL) was mixed with the EtOH (43.0 mL) with stirring for 30 min. Then, high purity water (1.0 mL) and ammonia (0.9 mL) were added to the solution and the mixture was stirred for 4 h. After stirring, the solution was transferred to a cool place to age for 7 days. After 7 days, the solution formed a sol. Then, EtOH (50 mL) was added to dilute the sol for later dip-coating.

The NH₃-OSER coatings were dip-coated on the cleaned glass substrates at the withdrawal rate 1.5 mm/s. Then, the samples were immersed in HMDS for 3 days to obtain a hydrophobic surface. Finally, the coated glasses were annealed in a muffle furnace at 160 °C for 1.5 h.

2.2.3. Preparation of the TEOS/MTES (TM) Coatings

TEOS (tetraethyl orthosilicate) (2.5 mL) and MTES (methyltriethoxysilane) (7.3 mL) were mixed with the EtOH (36.0 mL) with stirring for 30 min. Then, high purity water (1.3 mL) and ammonia (0.9 mL) were added to the solution and the mixture was stirred for 1 h. After stirring, the solution was transferred to a cool place to age for 7 days. After 7 days, the solution formed a sol. Then, EtOH (50 mL) was added to dilute the sol for later dip-coating.

The TM coatings were dip-coated on the cleaned glass substrates at the withdrawal rate 1.5 mm/s. Then, the samples were immersed in HMDS for 3 days to obtain a hydrophobic surface. Finally, the coated glasses were annealed in a muffle furnace at 160 °C for 1.5 h.

2.3. Characterization

The optical transmittance spectra of the coated glasses were measured by using a UV-VIS-NIR spectrophotometer (Hitachi U-4100, Tokyo, Japan) at room temperature. The refraction index and film thickness were measured by a spectroscopic ellipsometry (SENTECH SE800PV, Berlin, Germany). The surface morphologies and Young's modulus of the coatings were determined by atomic force microscope (Dimension Fastscan, Bruker, Billerica, MA, USA). The scratch resistance was evaluated by the pencil hardness test. The pencil hardness test was operated according to ASTM D 3363-2005. The optical microscope images of the scratches were taken by metallurgical microscope (LEICA DM2500M). FTIR spectra were recorded on the infrared spectrometer (Vertex70 Hyperion3000, with a diamond crystal plane (single reflection) Attenuated Total Reflection (ATR) attachment), with a resolution of 4 cm⁻¹ and range of 4000~400 cm⁻¹, to measure the possible groups on the coatings. Thermogravimetric analysis was performed by using thermogravimetry (TG209F1 libra) from 30 °C to 710 °C at a rate of 10 °C/min in the air to measure the decomposition temperature of the coating. The water contact angles were measured at

room temperature by an optical contact angle system (OCA 20, Dataphysics) with a droplet volume of 5 μL .

3. Results and Discussion

3.1. Formation Mechanism of the Double-Cross-Link Structure

The simple fabrication process of the coatings is schematically illustrated in Figure 1. For convenience, GPTES, DETA and MXDA are replaced by simple graphics in Figure 1a. In general, $\text{Si-O-C}_2\text{H}_5$ can be catalyzed by acids and alkalis to hydrolyze and produce silanol. At the same time, silanol can also be catalyzed to condense and produce Si-O-Si [4]. Aliphatic polyamine can also catalyze the hydrolysis and condensation of $\text{Si-O-C}_2\text{H}_5$, as discussed in the next section. Low-temperature epoxy groups ring-opening reaction and organic network formation can be achieved by the use of amine curing agents. In principle, each active hydrogen in an amine is capable of opening and linking to one epoxy groups [42]. That is, 1 mol of DETA react with 5 mol of GPTES and 1 mol of MXDA react with 4 mol of GPTES. Therefore, as shown in Figure 1b, DETA and MXDA not only catalyze the hydrolysis of $\text{Si-O-C}_2\text{H}_5$ and the condensation of silanol, but react with GPTES to form the double-cross-link network. As the reaction proceeds, the molecular chains gradually expand to achieve the much larger networks in Figure 1c,d (both amorphous from XRD, not present).

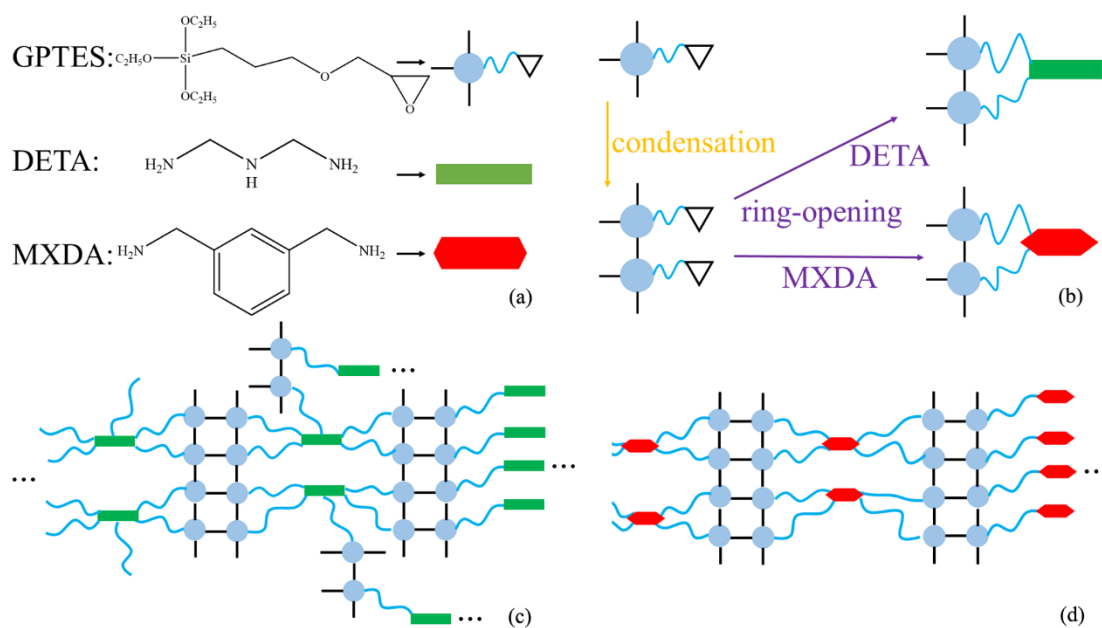


Figure 1. Schematic illustration of the OSER coating. (a) Simplification of reactant. (b) Reaction process. (c) DETA-OSER network. (d) MXDA-OSER network.

For the sake of verifying whether the cross-linked network was achieved, the FTIR spectrum was applied to infer the possible groups in coatings. Figure 2 shows FTIR spectra of NH_3 -OSER, MXDA-OSER, DETA-OSER and GPTES. Absorption peaks at ~ 2920 , ~ 2853 and $\sim 1457\text{ cm}^{-1}$ were observed corresponding to the C–H asymmetric, symmetrical stretching vibration and the in-plane deformation vibration, respectively [43]. This indicated that all the samples contained methylene. Moreover, the characteristic peak shown at $\sim 3292\text{ cm}^{-1}$ could be attributed to the stretching vibration of hydroxyl [44], including hydrogen bonds, which indicated that the $\text{Si-O-C}_2\text{H}_5$ in three coatings have hydrolyzed, whereas GPTES have not. Since the characteristic peak of O–H is very close to N–H, this might also suggest the existence of $-\text{NH}_2$. The characteristic peak shown at $\sim 910\text{ cm}^{-1}$ could be attributed to the vibration of epoxy. This indicated incompletely reacted epoxy groups. In addition, in terms of the characteristic peak shown at $\sim 1094\text{ cm}^{-1}$, which represented the Si–O stretching vibration [45], it could be confirmed that GPTES

contained unhydrolyzed Si–O–C₂H₅ and this peak corresponds to the cross-link networks of Si–O–Si in the other three samples. Furthermore, the presence of amino was observed at ~1649 and ~1025 cm⁻¹, and was assigned to the symmetric N–H bending modes of –NH₂ groups and C–N stretching modes of R₃N, respectively [45]. In other words, the open-ring reaction occurred between the GPTES and DETA or MXDA. On the contrary, GPTES was only catalyzed by ammonia to hydrolyze, but not ring-open. In summary, GPTES achieved the single Si–O–Si cross-link with the help of ammonia, but DETA and MXDA both catalyzed hydrolysis and condensation, and reacted with epoxy groups to produce the double cross-links Si–O–Si and R₃N.

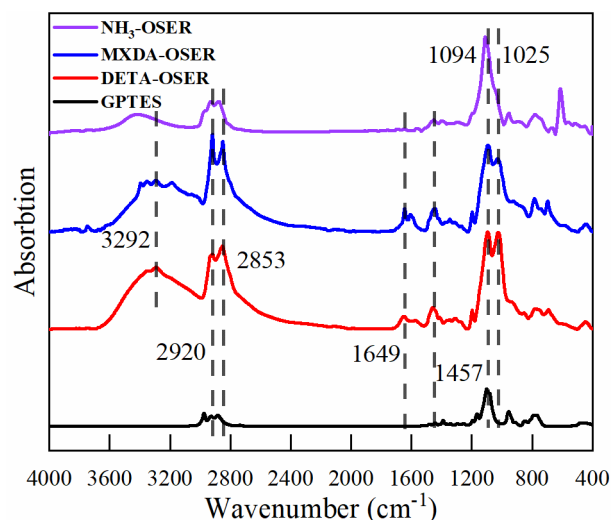


Figure 2. FTIR spectra of NH₃-OSER, MXDA-OSER, DETA-OSER and GPTES.

3.2. Mechanical Property of Coatings

Scratch resistance is an important property of coatings, especially the ones for optical applications. The hardness of the coatings was assessed by a pencil hardness test on the basis of the ASTM D3363 standard [46], using pencils ranging from 6B (the softest) to 9H (the hardest). As shown in Figure 3f, with MTES as the silane coupling agent, the TM coating had the softest pencil hardness < 6B, due to its low refractive index and high porosity. In fact, the hydrogen bonds among the methyl-embedded particles are weakened and the extent of cross-link is greatly reduced, leading to a high porosity [33]. The NH₃-OSER coating, using GPTES as the silane coupling agent, was also soft, which showed a pencil hardness < 3B, as Figure 3e. That means the single Si–O–Si cross-link is not strong enough to achieve ultra-scratch resistance. However, as shown in Figure 3a, there were only minor scratches on DETA-OSER, caused by an 8H pencil, yet it suffered evident scratch damage by 9H in Figure 3b. What is more, MXDA-OSER was also ultra-scratch resistant, absolutely none scratches on its surface as Figure 3c showed. In summary, owing to the double cross-links, the hardness of coatings is greatly enhanced to 8H. GPTES achieved the cross-link structure of Si–O–Si through hydrolysis and condensation because of ammonia, but this single cross-link was not very strong. The extent of the cross-link between the molecular chains is relatively weak, and there are still the possibility of slippage and dislocation under external force tearing. When introducing the curing agent, molecular chains are double cross-linked to each other, which strengthens the stability and robustness of the network and increases the relative molecular mass. Macroscopically, these make the polymer coatings rather hard, up to 8H. In fact, the extension of the double cross-link decides the hardness of the coating. As mentioned, each mole of active hydrogen in the amines react with one mole of epoxy group (H:epoxy = 1:1), theoretically. However, there is always a dynamic equilibrium in organic reaction, that is, not every epoxy group goes through a ring-opening reaction. In order to improve the conversion of epoxy groups, excessive curing agent is supposed to be added to the solution. According to Table 1, when

the proportion of hydrogen increased, the pencil hardness of both coatings also increased, proving that the excessive curing agent made the ring-opening reaction more thorough, and then the double cross-link network was strengthened. In detail, when the curing agent was less ($\leq 1:1$), the curing efficiency of DETA was higher, and the hardness reached to 5H. In other words, most GPTES was cured by DETA with a low concentration. As for MXDA, its small amount had a small increase in hardness. When H:epoxy = 2:1, the hardness of two coatings increased to 8H. However, the sol soon becomes a gel because of excessive curing in about 8 days. This is because the size of the cross-linked networks continues to expand as the aging time increases. Macroscopically, the fluidity of the sol is continuously weakened, and finally becomes a gel, making it impossible to go through the dip-coating process. So, the sol (epoxy:H = 1:2) needs to be diluted to slow down the growth of the cross-linked networks to prolong its life. According to experiments, when the concentration of sol was diluted to half, the sol was kept in a fluidized condition after 180 days.

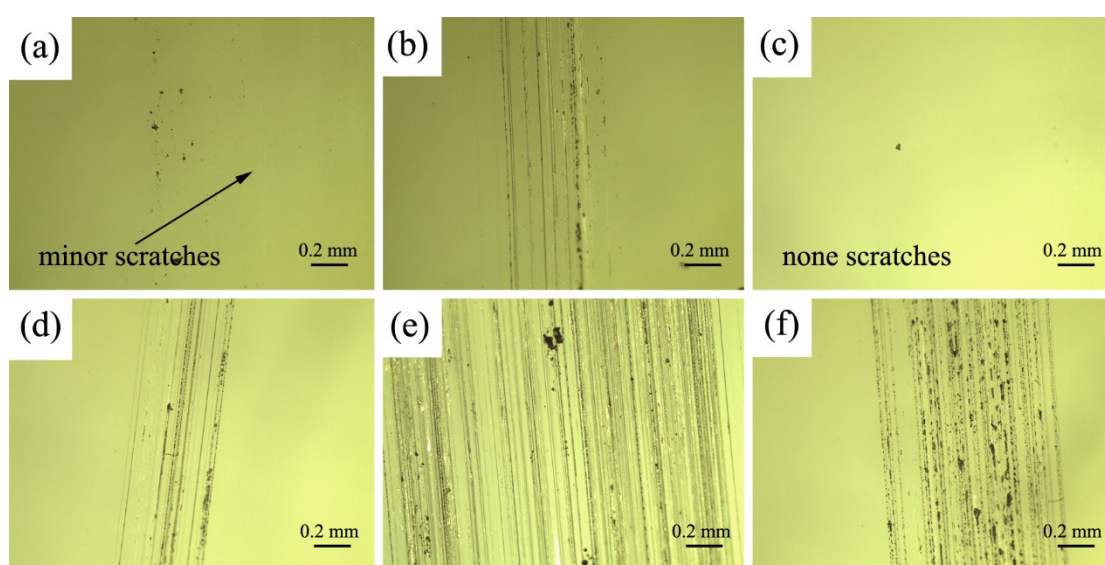


Figure 3. Optical microscope images of the scratches on various coatings. (a) DETA-OSER, scratched with an 8H pencil. (b) DETA-OSER, scratched with a 9H pencil. (c) MXDA-OSER, scratched with an 8H pencil. (d) MXDA-OSER, scratched with a 9H pencil. (e) NH_3 -OSER, scratched with a 3B pencil. (f) TM, scratched with a 6B pencil.

Table 1. Pencil hardness of DETA-OSER and MXDA-OSER in different molar ratios: H:epoxy.

	0.5	1.0	1.5	2.0
DETA-OSER	2H	5H	7H	8H
MXDA-OSER	3B	H	6H	8H

3.3. Morphology and Optical Property of Coatings

In order to confirm the hardness quantitatively and figure out the surface morphologies of the coatings, the coatings' Young's modulus and surface roughness were determined by atomic force microscope. Young's modulus describes the ability of a solid material to resist deformation. That is, the higher Young's modulus of the coating, the stronger its ability to resist bending and the greater its hardness. The black lines marked in Figure 4 are the center line average, which represents the average of Young's modulus of the coatings. The results shown in Figure 4 revealed that MXDA-OSER obtained the highest value of ~ 10.8 GPa, while TM obtained a minimum value of ~ 1.5 GPa. This result was approximately consistent with the scratch-resistance observation shown in Figure 3. The stability of the double cross-links structure was verified. Figure 5 showed the surface morphologies of the coatings. The corresponding root-mean-square deviation roughness (Rq) is given in

Figure 5. Spherical clusters on the surface could be observed as shown in Figure 5c,d. The roughness of NH₃-OSER and TM ($R_q = 2.024, 7.651 \text{ nm}$) was much higher than that of the DETA-OSER and MXDA-OSER ($R_q = 0.316 \text{ nm}, 0.274 \text{ nm}$). The result reflects that the DETA-OSER and MXDA-OSER had extremely smooth surfaces, which was attributed to their tightly linked molecular chains with double-cross-link structures. The smooth surface also greatly reduced the light scattering, resulting in a high transmittance of visible light. It is noticed that the scratch resistance of TM and NH₃-OSER was much weaker. Therefore, the further investigation on these two coatings will not be carried out.

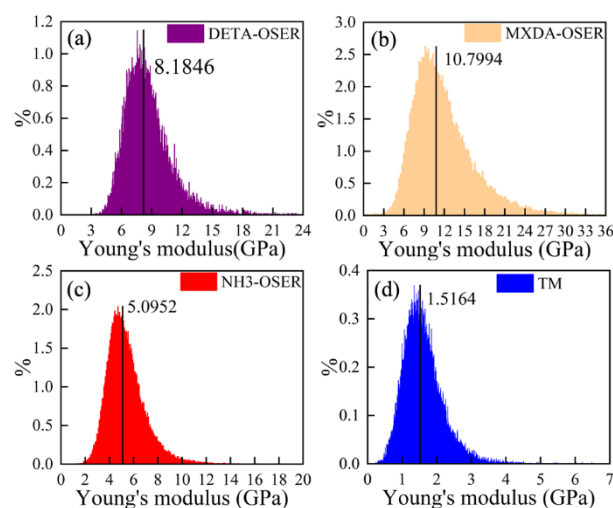


Figure 4. Histograms of the Young's modulus distribution of the coatings. (a) DETA-OSER. (b) MXDA-OSER. (c) NH₃-OSER. (d) TM.

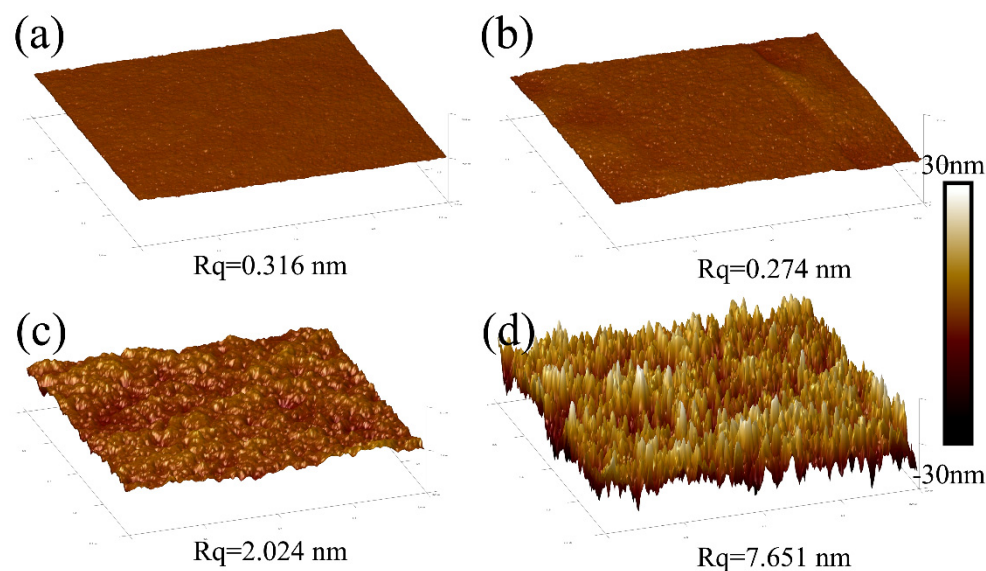


Figure 5. The 3D surface morphology of the coatings. (a) DETA-OSER. (b) MXDA-OSER. (c) NH₃-OSER. (d) TM.

According to Figure 6, the transmittance of the DETA-OSER was a little higher than that of bare glass. This slightly difference is caused by the refractive index. The refractive index and thickness of the coatings and glass, measured by spectroscopic ellipsometry, are given in Table 2. The result indicates that DETA-OSER can also be used as an antireflective coating. However, when using MXDA as a curing agent, phenyl was introduced into the molecular chains, which increased the density of particles in the molecular chains to a certain extent. Nevertheless, the large phenyl enhances the rigidity of the molecular

chains. Consequently, chains are more difficult to deform, curl and shift, which makes the coating extremely hard and ultra-scratch-resistant. Back to Figure 3c, there were no scratches, scratched with an 8H pencil, whereas in DETA-OSER, without phenyl, there were minor scratches on it. In a word, MXDA-OSER was more scratch resistant than DETA-OSER, but at the cost of a slight decrease in transmittance.

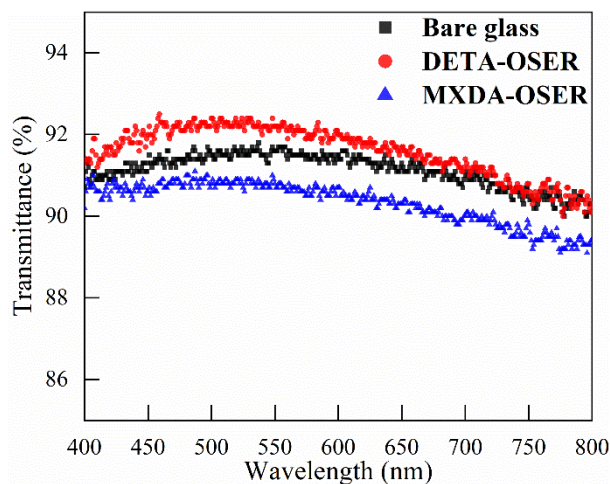


Figure 6. Transmittance spectra of the DETA-OSER, MXDA-OSER and bare glass.

Table 2. Refractive index and thickness of the DETA-OSER, MXDA-OSER and bare glass.

	Refractive Index (± 0.003)	Thickness
DETA-OSER	1.493	103 nm
Bare glass	1.512	700 μm
MXDA-OSER	1.525	114 nm

3.4. Durability in Different Environments of Coatings

The transmittance of coatings often decreases because of dust in practical applications. The coating with self-cleaning ability can effectively reduce the influence of dust on transmittance. Owing to being soaked in HMDS, the coating got the self-cleaning ability. Si-CH₃ in HMDS was transferred to the surface of the coating, making the surface hydrophobic. When the water droplet was dropped on the surface, the contact angle was up to 121°, which is shown in Figure 7b. However, in Figure 7a, the contact angle of the unsoaked DETA-OSER was just 69°, which was lower than the soaked one. It indicated that the hydrophobic groups were successfully grafted onto the surface. Additionally, this happened to MXDA-OSER. Generally, being soaked in the HMDS reduces the surface energy and increases the contact angle of water droplets, which endows the coating with self-cleaning ability.

The durability of the coating is a key technical concern. In order to study its chemical stability in different environments, DETA-OSER and MXDA-OSER were soaked in pH = 2 and pH = 12 solutions, seawater (3.5% NaCl aqueous solution) and organic solvent (anhydrous acetone), respectively. According to Tables 3 and 4, DETA-OSER and MXDA-OSER showed to be insoluble in acetone because their polarity was weak owing to the large molecular chains. Besides, DETA-OSER and MXDA-OSER, to a certain extent, could resist the erosion of the acid and seawater, but the hardness of DETA-OSER decreased slightly. The possible reason is that the molecular chains with phenyl are more inert due to the steric hindrance of phenyl. In addition, both DETA-OSER and MXDA-OSER could be soaked in an aqueous alkali only for a short time. The reason for hardness decline is that the Si-O-Si framework reacts with NaOH to produce the soluble Na₂SiO₃. Gradually, the corrosion of strong alkali destroyed the cross-link structure.

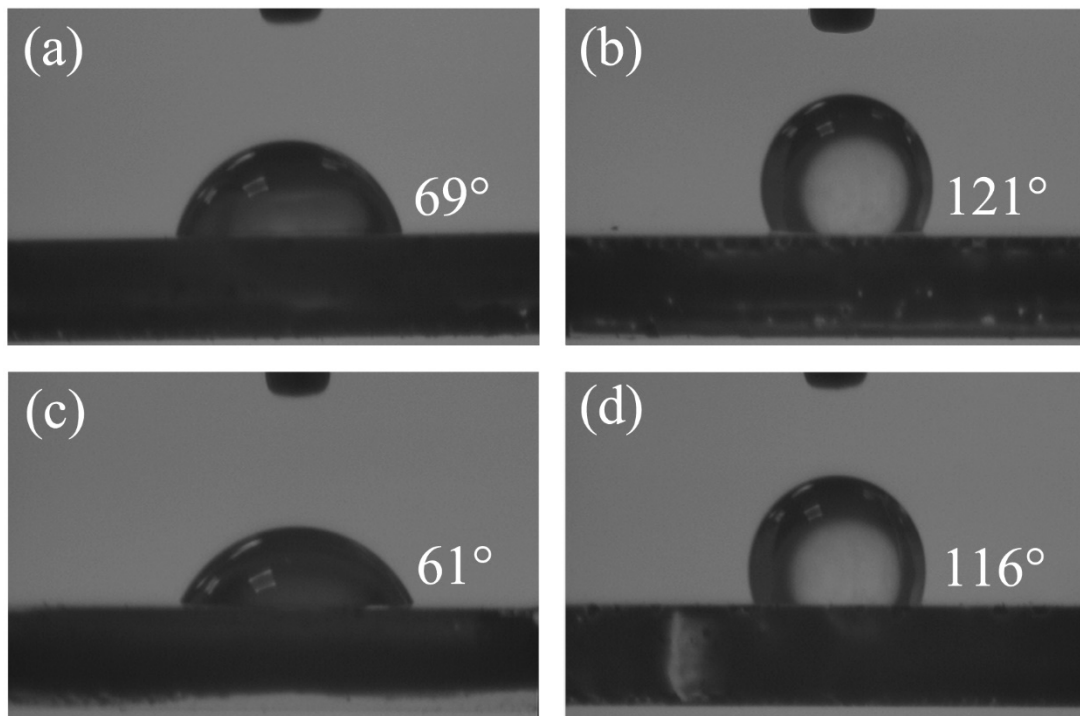


Figure 7. Contact angle of a water droplet on the surface of (a) DETA-OSER, before being soaked in HMDS. (b) DETA-OSER, after being soaked in HMDS. (c) MXDA-OSER, before being soaked in HMDS. (d) MXDA-OSER, after being soaked in HMDS.

Table 3. The pencil hardness grade of DETA-OSER being soaked in different solutions.

	1 Day	3 Days	5 Days	7 Days
pH = 2	8H	8H	8H	7H
pH = 12	8H	<6B	<6B	<6B
Seawater	8H	8H	8H	6H
Acetone	8H	8H	8H	8H

Table 4. The pencil hardness grade of MXDA-OSER being soaked in different solutions.

	1 Day	3 Days	5 Days	7 Days
pH = 2	8H	8H	8H	8H
pH = 12	8H	3B	<6B	<6B
Seawater	8H	8H	8H	8H
Acetone	8H	8H	8H	8H

To study the thermal behavior of materials, the thermal-oxidative decomposition processes of samples were investigated. According to the DTG curves shown in Figure 8, a maximum value with 160 °C and 13.4 min was observed. When the temperature was lower than 160 °C, the water adsorbed on the surface and started to evaporate, and the free Si–OH and the unreacted C₂H₅–O–Si also began to condense to produce a Si–O–Si cross-link structure, which reduced the mass during this time. In other words, annealing at 160 °C made the cross-link more thorough and then increased the hardness of the coating. When the temperature was higher than 160 °C, the rate of mass decrease began to increase, which meant that the polymer coating began to decompose intensely. Therefore, the DETA-OSER coating has the highest working temperature of 160 °C. Similarly, a maximum value of 155 °C was obtained at 12.7 min for MXDA-OSER coating. Meanwhile, it is observed that the DTG curves fluctuated greatly in the high-temperature region (>160 °C). This was

due to the fact that the coatings began to thermal decompose, producing gases such as CO_x , NO_x , NH_3 and alkanes with a different decomposition temperature and time.

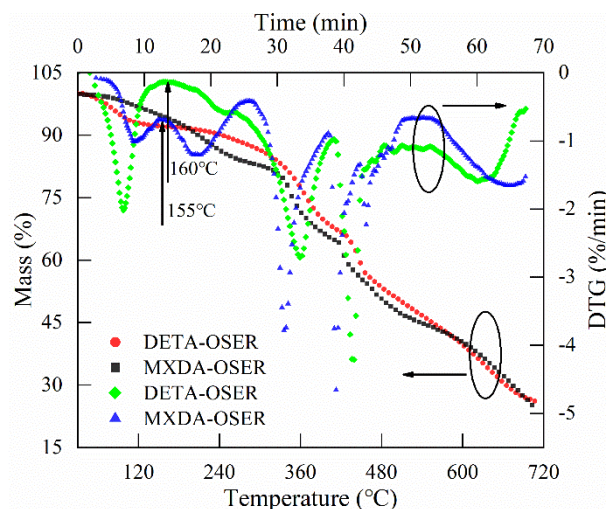


Figure 8. TGA and DTG curves of the samples of DETA-OSER and MXDA-OSER in air. The samples were made of the aged sol after drying the solvent at 60 °C, and they were not cured at a high temperature.

3.5. The Coating on Different Substrates

OSER can be applied on various substrates to protect the surface. The influence of the substrate on the scratch resistance was investigated. As shown in Figure 9, there were evident scratches on the coatings with a 9H pencil, but no scratches with an 8H, which meant that both DETA-OSER and MXDA-OSER were still ultra-scratch-resistant, even on iron substrates with a rough surface. Besides, owing to their inert and hydrophobic properties, OSER could be used as a protective coating to prevent the substrate from being scratched or becoming wet. Additionally, due to its high transparency, it had almost no effect on the pattern of the substrate.

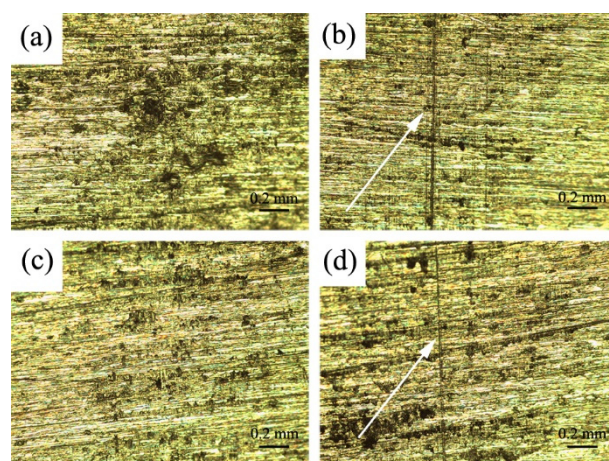


Figure 9. Surface morphologies of the OSERs on iron substrates after pencil hardness test. (a) DETA-OSER, scratched with an 8H pencil. (b) DETA-OSER, scratched with a 9H pencil. (c) MXDA-OSER, scratched with an 8H pencil. (d) MXDA-OSER, scratched with a 9H pencil.

4. Conclusions

In summary, we demonstrated a robust, hydrophobic and transparent coating based on organosilicon-epoxy resin (OSER). Aliphatic polyamines, as catalysts and reactants at the same time, make GPTES hydrolyze and condense as well as react with epoxy groups, thereby forming a double-cross-link structure. The double cross-links allow the coatings to resist scratching, macroscopically. The coating shows excellent scratch resistance and good

transparency. Besides, its durable and hydrophobic properties prevent the substrate from becoming wet by many solutions. The cost-effective coating exhibits great potential value in commercial applications.

Author Contributions: Conceptualization, Z.Q. and H.L.; methodology, Z.Q. and H.L.; formal analysis, Z.Q., L.Z. and Y.L.; investigation, Z.Q.; data curation, Z.Q.; writing—original draft preparation, Z.Q.; writing—review and editing, C.Z. and R.H.; visualization, Z.Q.; supervision, R.H.; project administration, R.H.; funding acquisition, R.H. All authors have read and agreed to the published version of the manuscript.

Funding: This research supported by Guangzhou Municipal Science and Technology Bureau (grant no. 201804020031) and Guangdong Basic and Applied Basic Research Foundation (grant nos. 2020A1515010057 and 2021A1515010626).

Acknowledgments: The authors gratefully acknowledge financial support from Guangzhou Municipal Science and Technology Bureau (grant no. 201804020031) and Guangdong Basic and Applied Basic Research Foundation (grant nos. 2020A1515010057 and 2021A1515010626).

Conflicts of Interest: The authors declare no conflict of interest.

References

1. Deng, X.; Mammen, L.; Butt, H.-J.; Vollmer, D. Candle Soot as a Template for a Transparent Robust Superamphiphobic Coating. *Science* **2012**, *335*, 67–70. [[CrossRef](#)] [[PubMed](#)]
2. Deng, X.; Mammen, L.; Zhao, Y.; Lellig, P.; Müllen, K.; Li, C.; Butt, H.-J.; Vollmer, D. Transparent, Thermally Stable and Mechanically Robust Superhydrophobic Surfaces Made from Porous Silica Capsules. *Adv. Mater.* **2011**, *23*, 2962–2965. [[CrossRef](#)] [[PubMed](#)]
3. Zhu, T.; Cheng, Y.; Huang, J.; Xiong, J.; Ge, M.; Mao, J.; Liu, Z.; Dong, X.; Chen, Z.; Lai, Y. A transparent superhydrophobic coating with mechanochemical robustness for anti-icing, photocatalysis and self-cleaning. *Chem. Eng. J.* **2020**, *399*, 125746. [[CrossRef](#)]
4. Cai, S.; Zhang, Y.L.; Zhang, H.L.; Yan, H.W.; Lv, H.B.; Jiang, B. Sol–Gel Preparation of Hydrophobic Silica Antireflective Coatings with Low Refractive Index by Base/Acid Two-Step Catalysis. *ACS Appl. Mater. Interfaces* **2014**, *6*, 11470–11475. [[CrossRef](#)]
5. Chevallier, P.; Turgeon, S.; Sarra-Bournet, C.; Turcotte, R.; Laroche, G. Characterization of Multilayer Anti-Fog Coatings. *ACS Appl. Mater. Interfaces* **2011**, *3*, 750–758. [[CrossRef](#)]
6. Brown, P.S.; Atkinson, O.D.L.A.; Badyal, J.P.S. Ultrafast Oleophobic-Hydrophilic Switching Surfaces for Antifogging, Self-Cleaning, and Oil-Water Separation. *ACS Appl. Mater. Interfaces* **2014**, *6*, 7504–7511. [[CrossRef](#)]
7. Chen, C.; Weng, D.; Mahmood, A.; Chen, S.; Wang, J. Separation Mechanism and Construction of Surfaces with Special Wettability for Oil/Water Separation. *ACS Appl. Mater. Interfaces* **2019**, *11*, 11006–11027. [[CrossRef](#)]
8. Mohammadkhani, R.; Ramezanzadeh, M.; Saadatmandi, S.; Ramezanzadeh, B. Designing a dual-functional epoxy composite system with self-healing/barrier anti-corrosion performance using graphene oxide nano-scale platforms decorated with zinc doped-conductive polypyrrole nanoparticles with great environmental stability and non-toxicity. *Chem. Eng. J.* **2019**, *382*, 122819.
9. Cho, E.C.; Chang-Jian, C.W.; Chen, H.C.; Chuang, K.S.; Zheng, J.H.; Hsiao, Y.S.; Huang, J.H. Robust Multifunctional Superhydrophobic Coatings with Enhanced Water/Oil Separation, Self-Cleaning, Anti-Corrosion, and Anti-biological adhesion. *Chem. Eng. J.* **2017**, *314*, 347–357. [[CrossRef](#)]
10. Ye, Y.; Zhang, D.; Liu, T.; Liu, Z.; Pu, J.; Liu, W.; Wang, L. Superior corrosion resistance and self-healable epoxy coating pigmented with silanized trianiline-intercalated graphene. *Carbon* **2018**, *142*, 164–176. [[CrossRef](#)]
11. Siddique, R.H.; Gomard, G.; Hoelscher, H. The role of random nanostructures for the omnidirectional anti-reflection properties of the glasswing butterfly. *Nat. Commun.* **2015**, *6*, 6909. [[CrossRef](#)]
12. Zhang, J.; Ai, L.; Lin, S.; Lan, P.; Lu, Y.; Dai, N.; Tan, R.; Fan, B.; Song, W. Preparation of humidity, abrasion, and dust resistant antireflection coatings for photovoltaic modules via dual precursor modification and hybridization of hollow silica nanospheres. *Sol. Energy Mater. Sol. Cells* **2019**, *192*, 188–196. [[CrossRef](#)]
13. Zhou, H.; Wang, H.; Niu, H.; Gestos, A.; Lin, T. Robust, Self-Healing Superamphiphobic Fabrics Prepared by Two-Step Coating of Fluoro-Containing Polymer, Fluoroalkyl Silane, and Modified Silica Nanoparticles. *Adv. Funct. Mater.* **2013**, *23*, 1664–1670. [[CrossRef](#)]
14. Dong, X.; Gao, S.; Huang, J.; Li, S.; Zhu, T.; Cheng, Y.; Zhao, Y.; Chen, Z.; Lai, Y. A self-roughened and biodegradable superhydrophobic coating with UV shielding, solar-induced self-healing and versatile oil-water separation ability. *J. Mater. Chem. A* **2019**, *7*, 2122–2128. [[CrossRef](#)]
15. Liang, B.; Zhong, Z.; Jia, E.; Zhang, G.; Su, Z. Transparent and Scratch-Resistant Antifogging Coatings with Rapid Self-Healing Capability. *ACS Appl. Mater. Interfaces* **2019**, *11*, 30300–30307. [[CrossRef](#)]
16. Banerjee, S.; Dionysiou, D.D.; Pillai, S.C. Self-cleaning applications of TiO₂ by photo-induced hydrophilicity and photocatalysis. *Appl. Catal. B* **2015**, *176*, 396–428. [[CrossRef](#)]

17. Latthe, S.S.; Sutar, R.S.; Kodag, V.S.; Bhosale, A.K.; Kumar, A.M.; Sadasivuni, K.K.; Xing, R.; Liu, S. Self-cleaning superhydrophobic coatings: Potential industrial applications. *Prog. Org. Coat.* **2019**, *128*, 52–58. [[CrossRef](#)]
18. Chattopadhyay, S.; Huang, Y.; Jen, Y.; Ganguly, A.; Chen, K.-H.; Chen, L. Anti-reflecting and photonic nanostructures. *Mater. Sci. Eng. R Rep.* **2010**, *69*, 1–35. [[CrossRef](#)]
19. Zhang, X.-X.; Xia, B.-B.; Ye, H.-P.; Zhang, Y.-L.; Xiao, B.; Yan, L.-H.; Lv, H.-B.; Jiang, B. One-step sol–gel preparation of PDMS–silica ORMOSILs as environment-resistant and crack-free thick antireflective coatings. *J. Mater. Chem.* **2012**, *22*, 13132–13140. [[CrossRef](#)]
20. Figueira, R.B.; Fontinha, I.R.; Silva, C.J.R.; Pereira, E.V. Hybrid Sol-Gel Coatings: Smart and Green Materials for Corrosion Mitigation. *Coatings* **2016**, *6*, 12. [[CrossRef](#)]
21. Chi, F.; Liu, D.; Wu, H.; Lei, J. Mechanically robust and self-cleaning antireflection coatings from nanoscale binding of hydrophobic silica nanoparticles. *Sol. Energy Mater. Sol. Cells* **2019**, *200*, 109939. [[CrossRef](#)]
22. Wang, Z.; van Andel, E.; Pujari, S.P.; Feng, H.; Dijkman, J.A.; Smulders, M.M.J.; Zuilhof, H. Water-repairable zwitterionic polymer coatings for anti-biofouling surfaces. *J. Mater. Chem. B* **2017**, *5*, 6728–6733. [[CrossRef](#)]
23. Wang, C.; Wu, H.; Chen, Z.; McDowell, M.T.; Cui, Y.; Bao, Z. Self-healing chemistry enables the stable operation of silicon microparticle anodes for high-energy lithium-ion batteries. *Nat. Chem.* **2013**, *5*, 1042–1048. [[CrossRef](#)]
24. Burnworth, M.; Tang, L.; Kumpfer, J.R.; Duncan, A.J.; Beyer, F.L.; Fiore, G.L.; Rowan, S.J.; Weder, C. Optically healable supramolecular polymers. *Nature* **2011**, *472*, 334–337. [[CrossRef](#)]
25. Nakahata, M.; Takashima, Y.; Yamaguchi, H.; Harada, A. Redox-responsive self-healing materials formed from host–guest polymers. *Nat. Commun.* **2011**, *2*, 511. [[CrossRef](#)]
26. Armaghani, D.J.; Mohamad, E.T.; Narayanasamy, M.S.; Narita, N.; Yagiz, S. Development of hybrid intelligent models for predicting TBM penetration rate in hard rock condition. *Tunn. Undergr. Space Technol.* **2017**, *63*, 29–43. [[CrossRef](#)]
27. Momeni, E.; Armaghani, D.J.; Hajihassani, M.; Amin, M.F.M. Prediction of uniaxial compressive strength of rock samples using hybrid particle swarm optimization-based artificial neural networks. *Measurement* **2015**, *60*, 50–63. [[CrossRef](#)]
28. Lu, Y.-X.; Guan, Z. Olefin Metathesis for Effective Polymer Healing via Dynamic Exchange of Strong Carbon–Carbon Double Bonds. *J. Am. Chem. Soc.* **2012**, *134*, 14226–14231. [[CrossRef](#)]
29. Amamoto, Y.; Otsuka, H.; Takahara, A.; Matyjaszewski, K. Self-Healing of Covalently Cross-Linked Polymers by Reshuffling Thiuram Disulfide Moieties in Air under Visible Light. *Adv. Mater.* **2012**, *24*, 3975–3980. [[CrossRef](#)]
30. Ji, S.; Cao, W.; Yu, Y.; Xu, H. Visible-Light-Induced Self-Healing Diselenide-Containing Polyurethane Elastomer. *Adv. Mater.* **2015**, *27*, 7740–7745. [[CrossRef](#)]
31. Cash, J.J.; Kubo, T.; Bapat, A.P.; Sumerlin, B.S. Room-Temperature Self-Healing Polymers Based on Dynamic-Covalent Boronic Esters. *Macromolecules* **2015**, *48*, 2098–2106. [[CrossRef](#)]
32. Hasanipanah, M.; Monjezi, M.; Shahnazar, A.; Jahed Armaghani, D.; Farazmand, A. Feasibility of indirect determination of blast induced ground vibration based on support vector machine. *Measurement* **2015**, *75*, 289–297. [[CrossRef](#)]
33. Zhang, Y.; Zhao, C.; Wang, P.; Ye, L.; Luo, J.; Jiang, B. A convenient sol–gel approach to the preparation of nano-porous silica coatings with very low refractive indices. *Chem. Commun.* **2014**, *50*, 13813–13816. [[CrossRef](#)] [[PubMed](#)]
34. Zhang, S.; Xiao, P.; Wang, P.; Luo, J.; Jiang, B. Spherical-chain silica with super-hydrophobic surface and ultra-low refractive index for multi-functional broadband antireflective coatings. *Sol. Energy* **2020**, *207*, 1222–1230. [[CrossRef](#)]
35. Mousavi, H.; Jilavi, M.H.; Koch, M.; Arzt, E.; De Oliveira, P.W. Development of a Transparent Scratch Resistant Coating through Direct Oxidation of Al-Coated Glass. *Adv. Eng. Mater.* **2017**, *19*, 1600617. [[CrossRef](#)]
36. Zhou, H.; Wang, H.; Niu, H.; Gestos, A.; Wang, X.; Lin, T. Fluoroalkyl Silane Modified Silicone Rubber/Nanoparticle Composite: A Super Durable, Robust Superhydrophobic Fabric Coating. *Adv. Mater.* **2012**, *24*, 2409–2412. [[CrossRef](#)] [[PubMed](#)]
37. Jin, F.-L.; Li, X.; Park, S.-J. Synthesis and application of epoxy resins: A review. *J. Ind. Eng. Chem.* **2015**, *29*, 1–11. [[CrossRef](#)]
38. Memon, H.; Liu, H.; Rashid, M.A.; Chen, L.; Jiang, Q.; Zhang, L.; Wei, Y.; Liu, W.; Qiu, Y. Vanillin-Based Epoxy Vitrimer with High Performance and Closed-Loop Recyclability. *Macromolecules* **2020**, *53*, 621–630. [[CrossRef](#)]
39. Tian, Y.; Wang, Q.; Shen, L.; Cui, Z.; Kou, L.; Cheng, J.; Zhang, J. A renewable resveratrol-based epoxy resin with high T_g, excellent mechanical properties and low flammability. *Chem. Eng. J.* **2020**, *383*, 123124. [[CrossRef](#)]
40. Zhi, J.; Zhang, L.-Z. Durable superhydrophobic surface with highly antireflective and self-cleaning properties for the glass covers of solar cells. *Appl. Surf. Sci.* **2018**, *454*, 239–248. [[CrossRef](#)]
41. Kesmez, Ö. Preparation of hybrid nanocomposite coatings via sol-gel method for hydrophobic and self-cleaning properties. *J. Mol. Struct.* **2020**, *1205*, 127572. [[CrossRef](#)]
42. Davis, S.R.; Brough, A.R.; Atkinson, A. Formation of silica/epoxy hybrid network polymers. *J. Non-Cryst. Solids* **2003**, *315*, 197–205. [[CrossRef](#)]
43. Grancaric, A.M.; Colleoni, C.; Guido, E.; Botteri, L.; Rosace, G. Thermal behaviour and flame retardancy of monoethanolamine-doped sol-gel coatings of cotton fabric. *Prog. Org. Coat.* **2017**, *103*, 174–181. [[CrossRef](#)]
44. Nazir, T.; Afzal, A.; Siddiqi, H.M.; Saeed, S.; Dumon, M. The influence of temperature and interface strength on the microstructure and performance of sol–gel silica–epoxy nanocomposites. *Polym. Bull.* **2011**, *67*, 1539–1551. [[CrossRef](#)]
45. Zhang, Y.; Zhang, X.; Ye, H.; Xiao, B.; Yan, L.; Jiang, B. A simple route to prepare crack-free thick antireflective silica coatings with improved antireflective stability. *Mater. Lett.* **2012**, *69*, 86–88. [[CrossRef](#)]
46. ASTM D3363; Standard Test Method for Film Hardness by Pencil Test. ASTM International: West Conshohocken, PA, USA, 2020. Available online: <https://www.astm.org/Standards/D3363.htm> (accessed on 15 September 2021).